Morphology of Gel-Spun Polyethylene Fibers

NASRIN KHOSRAVI,[1] S. B. WARNER,[2] N. S. MURTHY,[3] and SATISH KUMAR[1,*]

[1]School of Textile and Fiber Engineering, Georgia Institute of Technology, Atlanta, Georgia 30332-0295; [2]Department of Textile Sciences, University of Massachusetts, N. Dartmouth, Massachusetts 02742; [3]AlliedSignal Inc., P.O. Box 1021, Morristown, New Jersey 07962-1021

SYNOPSIS

Nitric acid etching studies have been conducted on samples of commercially available highly oriented gel-spun polyethylene fibers: Spectra™ 900 and 1000 from AlliedSignal Inc. The results show that the acid attacks the fiber, increases crystallinity as observed by X-ray diffraction, increases the enthalpy of melting of unconstrained fibers by 13–25%, and removes topological constrains thus facilitating the crystallization of chain segments in the noncrystalline regions. The acid functionalizes the fiber, creating various oxygen- and nitrogen-containing moieties, specifically (C=O)—, —C=C—, and —NO_2 groups. The small weight loss upon etching, less than 2%, and the fact that fibers weaken but do not fragment suggests that the gel-spun and -drawn morphology is more resistant to acid attack than are other morphologies of polyethylene. Photomicroscopy shows that acid etching opens cracks normal to the fiber axis. That the acid can attack the gel-spun fibers indicates the presence of structural imperfections such as folds, molecular kinks, or uncrystallized regions within the fibers. Infrared analysis on virgin fibers shows the absence of absorption bands normally associated with the presence of chains lying within amorphous regions in polyethylene. These and other morphological features are integrated into a description of the structure of commercial gel-spun polyethylene fibers. © 1995 John Wiley & Sons, Inc.

INTRODUCTION

Work on the crystallization of polyethylene from flowing solutions in the late 1960s and 1970s paved the way for the commercial development of gel-spun fibers from solutions of ultrahigh molecular weight polyethylene.[1-9] Typical properties of gel-spun polyethylene fibers are given in Table I.[8-10] The tensile strength of gel-spun UHMWPE fibers has been reported to be as high as 6 GPa,[9,11] which is more than half the "theoretical" value that is based on Monte Carlo simulations on model fibers.[12] The tensile modulus, reported to be as high as 220 GPa,[9,11] is even a greater fraction, two-thirds, of the theoretical value.[13] Because these fibers consist of a morphology that may begin to approach the ideal extended-chain continuous crystal, numerous research efforts have been directed toward elucidating the detailed microstructure of the fibers.[14-19]

Similar to the structure of all high modulus organic fibers,[20,21] the structure of gel-spun polyethylene is fibrillar. Thermal analysis on high modulus polyethylene fibers has been conducted by various research groups.[3,18,22,23] Gel spun fibers are characterized by multiple endothermic peaks that are readily observed using differential scanning calorimetry (DSC). The lowest melting endotherm peaks at about 143–148°C, a second endothermic transition occurs at about 150–155°C, and a final high-temperature melting endotherm appears at about 159–162°C.[3,22] The crystals, which may be envisioned as containing partially extended molecules, are connected by the ultralong chains. The connectivity among the crystals gives the polymer its high observed melting temperature.[24] This phenomenon is termed superheating. The superheating is caused by the difficulty of melting crystals into an isotropic melt from a state in which all of the molecules are highly extended and transgress extended chain

* To whom correspondence should be addressed.

Journal of Applied Polymer Science, Vol. 57, 781–787 (1995)
 CCC 0021-8995/95/070781-07

Table I Properties of Spectra Polyethylene Fibers

	Spectra™ 900	Spectra™ 1000
Density (g/cm^3)	0.97	0.97
Filament diameter (micrometers)	38	27
Tensile strength (GPa)	2.6	3.0
Tensile modulus (GPa)	117	172
Elongation to break (%)	3.5	2.7

crystals to pervade other crystals and oriented regions.[24,25]

All the peaks superheat to a large extent, as can also be seen simply by increasing the scan rate in the DSC.[3,24] The lowest-temperature melting endotherm is thought to be facilitated by sample changes that occur during heating in the DSC. Specifically, entropic shrinkage and recrystallization allow the endotherm to occur at a temperature lower than that characteristic of the same fibers heated while held at constant length. When fibers are constrained during DSC analysis, the 143–148°C endotherm may disappear altogether,[3,18,23] effectively shifting all endotherms to higher temperatures. The observation of an endotherm at about 160°C requires fiber constraint—intentional or not—during thermal analysis. The endotherm that occurs in the range of 150°C is attributed to a polymorphic (orthorhombic to hexagonal) transition.[3,23]

Nitric acid etching has been used extensively to gain additional insight into the morphology of various polyethylene samples.[3,26–29] Studies have been conducted on samples of polyethylene crystallized under quiescent conditions and on fiber formed using a Couette-type apparatus; however, experiments on gel-spun polyethylene fibers are lacking. The results show that hot nitric acid slowly attacks chain folds and facilitates removal of noncrystalline material. After nitric acid etching of lamellar crystals, the remaining polymer consists of rather short chains that are characteristic of the original crystal thickness.

In a comprehensive study, Pennings and Zwijnenburg investigated the effect of nitric acid etching on fibrillar crystals formed by longitudinal growth in a Couette-type apparatus.[3] These sorts of fibers were the predecessors to gel-spun fibers, but contain considerably more nonfibrillar crystalline material in the form of lamellar overgrowth. Pennings and Zwijnenburg showed that the heat of fusion of his fibers increased from about 252 to about 290 J/g with acid etching and that the fibers fragmented with etching. As mentioned previously, the gel-spun fiber has a different morphology; specifically, it lacks the lamellar-type overgrowth typical of fibers grown from a Couette-type apparatus. Nitric acid etching of commercially available gel-spun fibers was conducted in this study. After etching, the fibers were characterized by thermal analysis, infrared analysis, wide-angle X-ray diffraction, and scanning electron microscopy.

EXPERIMENTAL

The gel-spun fibers used in this investigation were kindly supplied by AlliedSignal Inc. The properties of Spectra™ 900 and 1000 supplied by the manufacturer are shown in Table I. Etching was conducted in a flask in fuming nitric acid at 65°C for a period of 50 and 100 h. To each milligram of fiber was added 100 mL of acid. Fiber samples removed from the nitric acid were washed in distilled water and dried in vacuum at 60°C for 48 h and weighed.

Thermal analysis was conducted using a Perkin-Elmer DSC-4, which was calibrated using indium. Fibers were cut into short lengths and 2–3 mg of fiber was crimped into aluminum pans. Scanning was conducted from 50 to 170°C at 1, 5, and 20°C/min. Each sample was cooled at 5°C/min to 50°C. Reheats were conducted at 20°C/min. Temperatures reported are peak temperatures. We conducted thermal analysis at various scan rates to probe the superheating effects; however, the heat of fusion at 20°C/min is used for determination of crystallinity, to minimize the effect of changes occurring in the fiber at slow heating rates. Heat of transition was computed by the instrumentation after a reasonable base line was established. Crystallinity was estimated using 293 J/g as the value for the heat of fusion of pure crystal.[30]

The values for crystallinity are subject to considerable error, as the imperfect crystals will be characterized by a heat of fusion of less than 293 J/g. In addition, proposed morphologies designed to accurately portray the structure of highly oriented polymers invariably contain three or more phases. Consequently, although we report crystallinity based on a two-phase morphology, the values are best considered to be a lower bound.

SEM photomicrographs were taken using a Hitachi S-800 microscope on samples sputter-coated to provide a gold–palladium coating of about 40 nm thick. A Perkin-Elmer Fourier transform infrared spectrophotometer 1620 equipped with a transmitted beam infrared microscope attachment without a po-

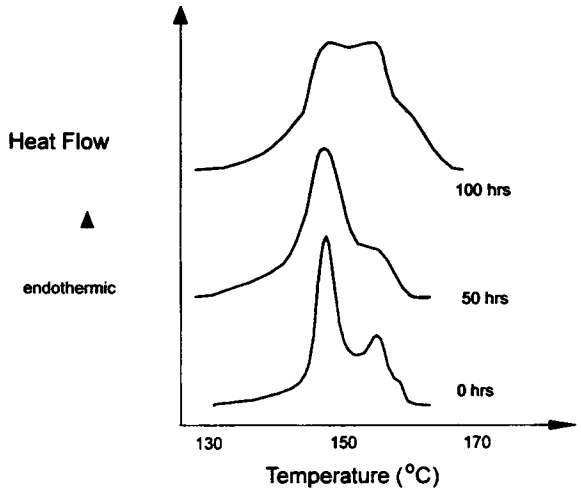

Figure 1 Thermal analysis of Spectra 1000: (a) effects of heating rate on the virgin fiber; (b) effects of nitric acid etching for various times (heating rate 20°C/min).

larizer was used to examine Spectra fibers for chemical changes after etching. IR spectra were collected on virgin and etched fibers. Polyethylene film was used as a reference material.

X-ray diffraction data were collected using a Philips powder diffractometer. The fiber was wound on a frame to cover a 1 cm window. Data were collected in the 2θ range of 10–35°. Equatorial scans were collected to obtain the lateral crystallite size using the Scherrer equation: crystallite size = $0.9\ \lambda/(B\ \mathrm{Cos}\ \theta)$, where λ is the X-ray wavelength (1.54 Å in the present case), and B, the full width at half-maximum of the peak. The peaks were modeled as Gaussian and the widths were corrected for instrumental broadening. For crystallinity measurements, the frame was spun in its plane so as to randomize the orientation of the fiber. The ratio of the area under the crystalline peaks to the total scattered intensity was used to calculate the crystallinity of the fiber.[31] In preliminary studies, peak shapes were fitted using Lorentzian and modified Lorentzian shapes; however, using these peak shapes, the data did not fit well. Much better fit was obtained using Gaussian peak shapes. We include some data from the Lorentzian analysis to show the large difference in crystallinity that results from the use of different peak shapes.

RESULTS AND DISCUSSION

The effect of the heating rate on the thermal behavior of Spectra 1000 is shown in Figure 1. Each of the three endothermic peaks show superheating effects. These results are consistent with those reported in other studies.[3] The cooling curve is characterized by a single crystallization exotherm that peaks at 113–121°C and the remelt curve by a single endothermic peak at 131–142°C. The melt temperature, heat of fusion, and calculated crystallinity of nitric acid etched gel-spun fibers are given in Table II. Close examination of the data suggest the following:

1. The crystallinity increases with etching time. Using a value of 293 J/g for the heat of fusion of the polyethylene crystal, the crystallinity in Spectra 1000 is calculated to be about 77%. The crystallinity in the etched sample is about 87%. Spectra 900 shows an increase from about 69% to about 87% with nitric acid etching. These values may be usefully compared to those reported in other studies and cited below for X-ray diffraction results. Based on solid-state nuclear magnetic resonance studies, Tzou et al. reported the presence of two crystalline phases, C_1 and C_2, in Spectra.[19] In Spectra 900, C_1 and C_2 are 6 and

Table II Properties of Gel-spun Polyethylene Fibers Before and After Nitric Acid Etching[a]

Sample	Melting Temperature (°C)	Heat of Fusion (J/g)	DSC Crystallinity (%)	Heat of Crystallization (J/g)
Spectra 1000	148, 156, 159	225	77	143
Etched 50 h	148, 155	244	83	139
Etched 100 h	148, 152, 159	256	87	147
Spectra 900	146, 155	203	69	118
Etched 50 h	142, 155	241	82	160
Etched 100 h	142	256	87	168

[a] Etching temperature 65°C; heating rate in DSC 20°C/min.

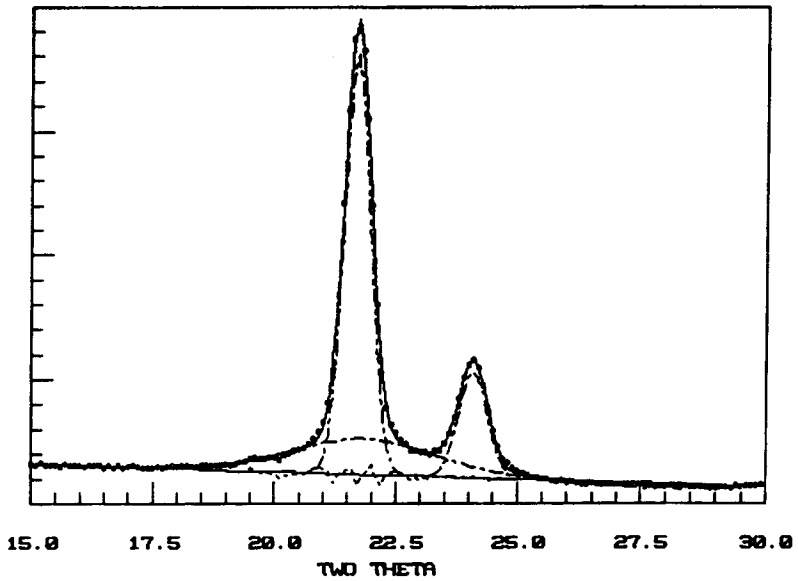

Figure 2 Wide-angle X-ray diffraction of virgin and nitric acid-treated gel-spun polyethylene fiber: (a) virgin Spectra 1000 fiber; (b) Spectra 1000 fiber after 100 h etching.

76% of the polymer, respectively, the balance being unoriented noncrystalline polymer. In Spectra 1000, C_1 and C_2 are 15 and 85%. Pennings and Zwijnenburg etched Couette-produced fibers.[3] Prior to etching, the crystallinity was about 88%, and with etching, the crystallinity increased to 99%. Our results suggest that, unlike in Pennings and Zwijnenburg's work, the nitric acid may not be able to reach and react with all the noncrystalline polymer, folds, ends, or defects. This may be, in part, due to the high percent crystallinity and very high orientation of the noncrystalline regions, which reduces the ability of fluids and gases to penetrate and diffuse through polymers, or may be due to the presence of noncrystalline material as discrete regions in a continuous crystalline matrix, or both.

2. The increased heat of crystallization with etching is likely a result of molecular weight reduction. Molecular weight reductions have also been observed on polyethylenes that are susceptible to a considerable extent of nitric acid attack, such as those containing lamellar crystals.[26-29]

The increase in crystallinity with nitric acid etching is consistent with the results of others;[3,26-29] however, our samples showed a remarkably small weight loss. Only 0.13 and 1.61 wt % of Spectra 1000 and 900, respectively, were lost after 50 h etching. This result suggests that few of the chains are actually removed from the fibers during etching; rather, the molecules are attacked by the acid at regions of local susceptibility, but the cleaved chains remain largely in place. Cleaving of the chains at defects may reduce residual stresses and may provide the oriented molecules with sufficient mobility to crystallize. Hence, crystallinity increases without weight loss can be understood. Weight loss by etching in a very small part is also counterbalanced by the addition of nitrogen and oxygen to the polymer chain, which is consistent with IR data.

Typical X-ray diffraction scans from the control fiber and the nitric acid etched fibers are shown in Figure 2 and the results are summarized in Table III. The invariance of the (110) and (200) peak positions with etching time shows that the crystal structure does not change with the etching process. The measurements of crystallinity by X-ray confirm the increase in crystallinity (by DSC) with etching time. The results show that crystallinity increases from about 69 to 73% with etching in Spectra 1000 and from 65 to 70% in Spectra 900. (The magnitude of crystallinity based on a Lorentzian peak fit analysis is surprisingly larger than that based on the better-fitting Gaussian analysis. Using a Lorentzian model, the crystallinity in Spectra 1000, 100%, is invariant with etching time. In Spectra 900, on the other hand, it increases from 89 to 93% with 100 h etching. These differences between the two analyses demonstrate that crystallinity is extremely sensitive to the details of the X-ray data analysis technique.)

The difference in crystallinity determined by X-ray and DSC techniques is not unusual; rather, it is typical. Each technique is based on a rather simplistic assumption of a two-phase morphology. Moreover, oriented noncrystalline materials is especially difficult to reconcile with either model. The minimal weight loss of Spectra 1000 with nitric acid etching suggests that the major affect of the chain cleavage by the acid is to remove the topological constraints and thus facilitate crystallization of the chain segments in noncrystalline regions.

The results of infrared analysis are shown in Figure 3. Absorbances at the 650–730 wavenumbers are due to CH_2 rocking; 1470, to CH_2 bending; and 2900, to CH stretching. The absorbance assigned to C=O in the film is likely due to the presence of surface oxidation, fillers, or both. Absorbances at 1240, 1303, and 1368 wavenumbers are evidence of noncrystalline regions in polyethylene.[32] These amorphous bands are strong in the film, while the gel-spun fibers show no absorption at the frequencies corresponding to the presence of amorphous regions. This suggests that the noncrystalline polymer exists in a different form in Spectra than in melt-processed polyethylene. Perhaps, noncrystalline polymer is present as essentially isolated loops, folds, or defects. Or, more likely, molecules with largely *trans* configuration are present, yet remain uncrystallized because of misalignment with other molecules or because residual stresses prevent lattice registry.

Spectra fibers that have been subjected to nitric acid etching show absorbances at 1558, 1633, and 1718 wavenumbers, which are due to the presence of $-NO_2$, $-C=C-$, and $-(C=O)-$moieties. This result is in agreement with previous work based on diffuse transmission FTIR spectroscopy, which was conducted on Spectra fibers etched with nitric acid to improve their adhesion with matrices in composites.[33]

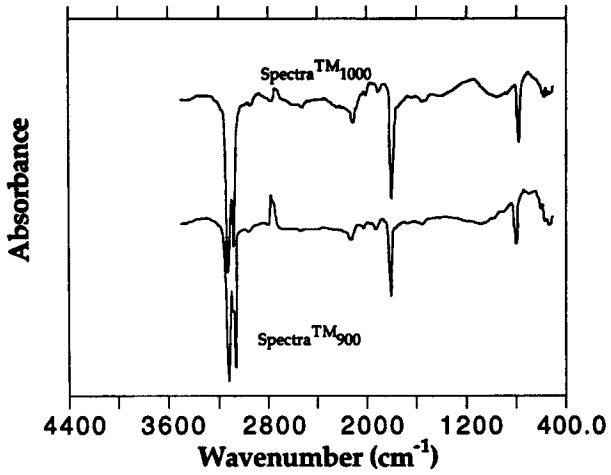

Figure 3 Infrared analysis on virgin and nitric acid-treated gel-spun polyethylene fiber: (a) spectra of virgin fibers and polyethylene film standard; (b) spectra of nitric acid-etched fibers.

SEM analysis of the etched and dried fibers show that cracks have developed normal to the fiber axis, as shown in Figure 4. That the etchant was able to get a foothold in the fiber is indicative of imperfections in the fiber: that there are high-energy sections along the molecules, perhaps chain folds, noncrystalline polymer, or other strained and vulnerable regions of the fiber. The morphology of the etched fiber, however, is likely a result of the release of entropic stresses within the fiber. Both chemical and ion etching of various fibers have given rise to structures that relate more to etching conditions than to fiber morphology. Structures similar to those shown in Figure 4, e.g., have been observed on ion-etched

Table III X-ray Diffraction Data

Sample	Crystallinity[a] (%)	Diffraction Angle, 2θ (110) (°)	Diffraction Angle, 2θ (200) (°)	Crystallite Size[b] (110) (Å)	Crystallite Size[b] (200) (Å)
Spectra 1000	69	21.5	23.9	142	128
Etched 50 h	75	21.5	23.9	137	123
Etched 100 h	73	21.5	23.9	140	128
Spectra 900	65	21.5	23.9	131	120
Etched 50 h	70	21.5	23.9	133	111
Etched 100 h	70	21.5	23.9	140	121

[a] From a rotational scan, assuming a two-phase morphology and a Gaussian diffraction peak shape.
[b] From equatorial scan after instrumental broadening correction.

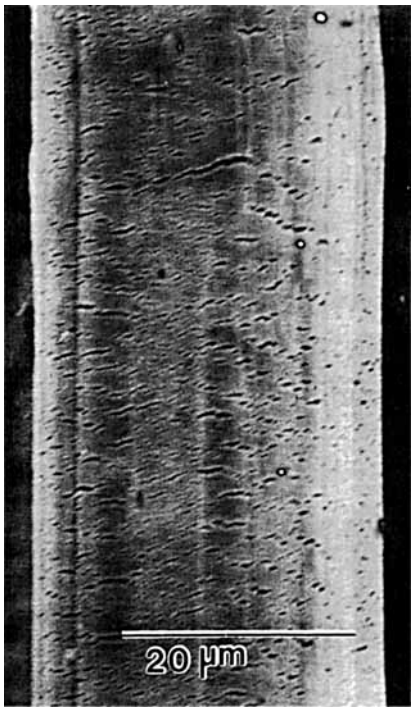

Figure 4 Scanning electron micrograph of 100 h nitric acid-etched Spectra 1000 polyethylene fiber.

acrylic fibers,[34] hypochlorite-etched acrylic fibers,[35] and amine-etched polyester fibers.[36] Thus, we are reluctant to attribute specific morphological features in the gel-spun fiber to the etching disfiguration. That the etchant had any effect, however, is clearly indicative of heterogeneities in the structure, perhaps chain defects such as strain energy, loops, and folds if not (highly oriented) noncrystalline regions.

CONCLUSIONS

Crystallinity, as measured by DSC and by wide-angle X-ray diffraction, increases on nitric acid etching. The noncrystalline material in Spectra does not absorb at the usual infrared frequencies associated with amorphous regions in polyethylene, suggesting that it is unlike noncrystalline material in melt-processed samples of polyethylene and it may readily crystallize when "defects" are cleaved. In addition, noncrystalline polymer is at the least highly oriented and constrained by the crystalline network and may exist in isolated discrete regions. Nitric acid etching removes topological constraints and facilitates crystallization of chain segments in the noncrystalline regions. SEM examination suggests the heterogeneities associated with the susceptibility to nitric acid attack lead to transverse cracking in the fiber.

The authors gratefully acknowledge the experimental assistance of V. R. Mehta, C. P. Chang, and H. Minor.

REFERENCES

1. A. J. Pennings, *Crystal Growth, Proceedings of the International Conference on Crystal Growth,* H. S. Peiser, Ed., Pergamon Press, New York, 1967, p. 389.
2. A. J. Pennings, C. J. H. Schouteten, and A. M. Kiel, *J. Polym. Sci. C,* **38,** 167 (1972).
3. A. J. Pennings and A. Zwijnenburg, *J. Polym. Sci. Polym. Phys. Ed.,* **17,** 1011–1032 (1979).
4. J. Smook and A. J. Pennings, *J. Appl. Polym. Sci.,* **27,** 2209 (1982).
5. J. Smook and A. J. Pennings, *J. Mater. Sci.,* **19,** 31 (1984).
6. P. F. Van Hutten, C. E. Koning, and A. J. Pennings, *J. Mater. Sci.,* **20,** 1556 (1985).
7. W. Hoogsteen, R. J. Van den Hooft, A. R. Postema, G. ten Brinke, and A. J. Pennings, *J. Mater. Sci.,* **23,** 3459 (1988).
8. P. Smith and P. J. Lemstra, *J. Mater. Sci.,* **15,** 505 (1980).
9. S. Kavesh and D. C. Prevorsek, U. S. Pat. 4,413,110 (1983).
10. B. Poulaert, J.-C. Chielens, C. Vandenhende, J.-P. Issi, and R. Legras, *Polym. Commun.,* **31,** 148 (1990).
11. J. C. M. Torfs, and A. J. Pennings, *J. Appl. Polym. Sci.,* **26,** 30 (1981).
12. Y. Termonia, P. Meakin, and P. Smith, *Macromolecules,* **18,** 2246 (1985).
13. S. G. Wierschke, *Mater. Res. Symp. Proc.,* **134,** 313 (1989).
14. H. D. Chanzy, P. Smith, J.-F. Revol, and R. St. John Manley, *Polym. Commun.,* **28,** 133 (1987).
15. B. J. Kip, C. P. Van Ejik, and R. J. Meier, *J. Polym. Sci. Part B Polym. Phys.,* **29,** 99 (1991).
16. K. Prasad and D. T. Grubb, *J. Polym. Sci. Part B: Polym. Phys.,* **28,** 2199 (1990).
17. D. Hofmann, E. Schulz, and E. Walenta, *Acta Polym.,* **41,** 371 (1990).
18. A. W. Saraf, P. Desai, and A. S. Abhiraman, *J. Appl. Polym. Sci. Appl. Polym. Symp.,* **47,** 67 (1991).
19. D.-L. Tzou, T.-H. Huang, A. S. Abhiraman, and P. Desai, *Polymer,* **33,** 426 (1992).
20. L. C. Sawyer, and M. Jaffe, *J. Mater. Sci.,* **21,** 1897 (1987).
21. S. Kumar, in *International Encyclopedia of Composites,* S. M. Lee, Ed., VCH, New York, 1991, Vol. 4, p. 51.
22. D. Zenke, R. Hirte, and P. Wiegel, *J. Therm. Anal.,* **33,** 1171 (1988).
23. N. S. Murthy, S. T. Correale, and S. Kavesh, *Polym. Commun.,* **31,** 50 (1990).
24. B. Wunderlich and G. Czornyi, *Macromolecules,* **10,** 996 (1987).
25. J. Clement and I. M. Ward, *Polymer,* **23,** 935 (1982).

26. R. P. Palmer and A. J. Cobbold, *Makromol. Chem.*, **74,** 174 (1964).
27. G. Meinel and A. Peterlin, *J. Poly. Sci. Part A2,* **6,** 587 (1968).
28. K. H. Illers, *Makromol. Chem.*, **118,** 88 (1968).
29. F. M. Willmouth, A. Keller, I. M. Ward, and T. Williams, *J. Polym. Sci. Part A2,* **6,** 1627 (1968).
30. B. Wunderlich, *Macromolecular Physics,* Academic Press, New York, 1973, Vol. 1, p. 388.
31. N. S. Murthy and H. Minor, *Polymer,* **31,** 996 (1990).
32. P. C. Painter and J. L. Koenig, *J. Polym. Sci. Polym. Phys. Ed.,* **15,** 1223, 1235 (1977).
33. A. Taboudoucht, R. Opalko, and H. Ishida, *Polym. Compos.,* **13,** 81 (1992).
34. S. B. Warner, D. R. Uhlmann, and L. H. Peebles, Jr., *J. Mater. Sci.,* **10,** 758 (1975).
35. J. Herms, L. H. Peebles, Jr., and D. R. Uhlmann, *J. Mater. Sci.,* **18,** 2517 (1983).
36. R. Murray, H. A. Davis, and P. Tucker, *Appl. Polym. Symp.,* **33,** 177 (1978).

Received January 16, 1995
Accepted February 17, 1995